DEM STUDY ON THE DYNAMIC PERFORMANCE OF A FOULED BALLASTED TRACK UNDER REPEATED TRAFFIC LOADING

Jing Chen[1], Buddhima Indraratna[2], Jayan S. Vinod[3], Ngoc Trung Ngo[2], Yangzepeng Liu4[4]

[1] Department of Civil Engineering, Zhejiang University, China
[2] Transportation Research Centre, Faculty of Engineering and Information Technology, University of Technology Sydney, Australia
[3] Faculty of Engineering and Information Sciences, University of Wollongong, Australia
[4] China Railway 11th Bureau Group Co Ltd, China

Abstract. The fouling of ballast, resulting from upward intrusion of subgrade slurries, coal or other mineral ore dislodging from passing freight traffic, and the accumulation of debris among ballast grains, has been extensively reported as the primary cause for numerous disastrous railroad incidents. This paper presents a numerical study to examine the deformation and degradation responses of a coal-fouled ballasted track upon repeated traffic loading using the discrete element modeling (DEM). A particle degradation model considering Weibull statistics in tandem with a granular medium size effect is developed and employed to capture the continuous corner abrasion of angular ballast. The model had been calibrated by comparing the predicted shear stress-strain response with laboratory data obtained from large-scale direct shear testing. A series of cubical shear test simulations have been carried out to examine the dynamic performance of ballast assemblies with various coal fouling contents under cyclic loading. The results show that an increase in fouling content exacerbates the sleeper settlement, while decreasing the resilient modulus and the particle breakage in ballasted bed. Ballast beneath the sleeper experiences significant breakage compared to the crib ballast, and the extent of damage is mitigated with depth. Rigorous microscopic analysis is also presented in terms of inter-particle contacts and contact network anisotropy of the ballast assembly. The micro-mechanical examinations show that the decrease in ballast breakage observed in fouled assemblies is predominantly attributed to the inevitable decrease in inter-particle pressures as effected by the coating of ballast aggregates by the coal fines.

Keywords: Fouling, Ballast Breakage, Settlement, Discrete Element Method

1 Introduction

Ballasted railways are one of the most common transportation forms worldwide owing to their low construction cost, high environment adaptability, and efficient travel capabilities. The key components of ballasted tracks include a ballast layer and superstructure consisting of sleepers, rails, fastening system, and more. As traffic volume

increases, the ballast aggregate undergoes inevitable degradation through the breakage of individual particles and contamination by external fines like subgrade slurry, coal dust from passing trains, and sleeper debris. The fouling of the ballast layer has been identified as a fundamental cause of various track issues, such as impaired drainage, differential sleeper settlement, and rail buckling. These problems pose a significant threat to track safety and require substantial annual maintenance expenditures.

The mechanical properties of fouled ballast have been extensively examined by railway researchers. Tennakoon et al. [1] investigated the detrimental effect of fouling fines on the hydraulic conductivity of rail substructure. By conducting large-scale triaxial test on clean and clay-fouled ballast, Tennakoon and Indraratna [2] explored the impact of clay fouling on the stress-strain behavior, resilient modulus and degradation of ballast. Huang et al. [3] examined the shear strength of ballast aggregates fouled by different fouling agents including clay, coal dust, and mineral filler, and found that coal dust played the most detrimental effect on the shear strength of ballast. Tutumluer et al. [4] conducted a series of direct shearing test on ballast aggregates contaminated by coal dust at different percentages by weight and moisture contents. Their study found that the friction angle of ballast fully fouled with wet coal dust at 35% moisture content was close to the friction angle of coal dust itself, which has been identified as the worst fouling scenario in the field. Danesh et al. [5] investigated the effect of sand and clay fouling on the shear strength of railway ballast with different size gradations.

There are studies trying to explore the fundamental influencing mechanism of fouling agents on the mechanical behavior of ballast by using the numerical approach, among which the discrete element method (DEM) [6] is the most prevailing. By leveraging DEM modelling, Huang and Tutumluer [7] simulated the fouled ballast behavior under direct shearing conditions. However, the effect of fouling fines was indirectly achieved by a reduced friction coefficient of ballast. An alternative and more direct method which adds small sized elements in ballast voids to represent fouling materials was proposed by Indraratna et al. [8]. By utilizing this approach, Ngo et al. [9] investigated the influence of fouling fines on the reinforcement effect of geogrid to ballast aggregates. Chen et al. [10] studied the stress-dilatancy response of ballast fouled by coals and clay soils. Xu et al. [11] established a track model in DEM and examined the influence of fouling fines on the lateral resistance of ballast beds.

Most of the abovementioned studies were on a representative volume element of ballast, which failed to consider the interaction between ballast and overlying superstructures (i.e., sleepers). The mechanical behavior of ballast in real track fields still remains unclear. In addition, the degradation of ballast particles was not incorporated in the existing DEM studies, which hinders the investigation of the effect of fouling materials on the degradation behavior of ballast aggregates. Given the status-of-quo, DEM models simulating a representative ballasted track section under various fouling levels were established. Cyclic traffic loading was applied onto the track model, whereby the deformation and degradation behavior of ballast aggregates were examined. Micromechanical response in terms of the interparticle behavior was investigated to explore the fundamental influencing mechanism of fouling materials on ballasted tracks.

2 Large-scale cubical box test

In order to model the interaction between ballast aggregates and the overlying sleepers and to replicate the stress conditions experienced by ballast in actual rail tracks, an innovative Track Process Simulation Apparatus (TPSA) was developed by Indraratna et al. [12] at the University of Wollongong, Australia. This apparatus was designed for conducting large-scale cubical box tests (CBT) on ballast. Unlike conventional laboratory tests such as the direct shear test (DST) or triaxial compression test (TCT), the large-scale CBT includes a section of the sleeper and a ballast layer with the same depth as that found in real track fields. In this study, the large-scale CBT on clean and coal-fouled ballast was simulated by using the DEM. This section provides the details of the track model, the testing program, as well as the model calibration and validation.

2.1 Clean and fouled ballasted track model

Ballast is characterized by its irregular shape, which significantly influences the mechanical properties of aggregates. In order to replicate the shape irregularity of ballast grains, the CT-scanning technique in combination with the overlapping-sphere approach was utilized to create clump particles that closely resemble real ballast particles. Fig. 1(a) shows the images of five typical ballast grains and their corresponding clump particles in the current DEM analysis. Coal fouling was simulated as rigid spheres with varying sizes.

Fig. 1(b) shows an image of a typical ballasted track model established in this study. The dimensions of the model were 600 mm (L) × 300 mm (W) × 450 mm (H). In rail track, the spacing between two adjacent sleepers is normally 600 mm, which can be regarded as the minimum unit of the tracks. As the current study focuses on ballast behavior along the depth of track beds, only a width of 300 mm was selected along the transverse direction of sleepers considering computational efficiency. The depth of bottom ballast was 300 mm, above which a sleeper simulated by rigid wall element was placed. The sleeper was surrounded by crib ballast having a thickness of 150 mm. The sizes of ballast clumps ranged from 12 mm to 65 mm, with the particle size distribution (PSD) complying with AS 2758.7. The porosity of clean ballast aggregate was 0.43, which was similar to that measured in actual rail fields.

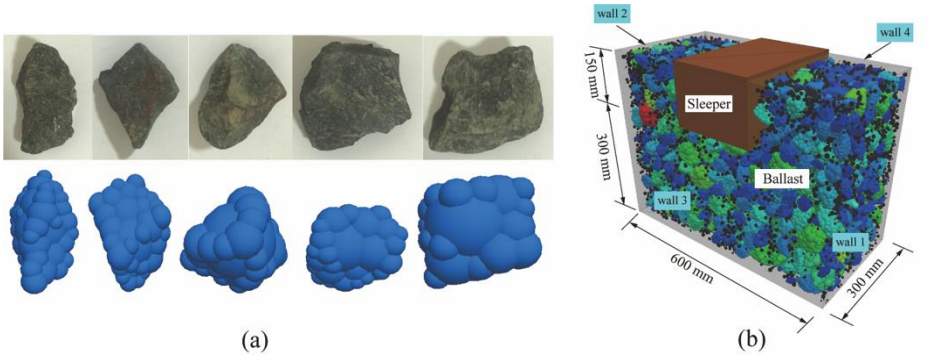

Fig. 1. (a) typical ballast particles and DEM clumps; (b) coal fouled ballasted track model

The Void Contamination Index (VCI) proposed by Tennakoon and Indraratna [2] was adopted to quantify the amount of coal fouling, as given by:

$$\mathrm{VCI} = \frac{1+e_f}{e_b} \times \frac{G_b}{G_f} \times \frac{M_f}{M_b} \times 100\% \quad (1)$$

where e_b and e_f are the void ratios of ballast and coal fouling, respectively; G_b and G_f are the specific gravities of ballast and coal fouling, respectively; M_b and M_f are the dry masses of ballast and coal fouling, respectively. To represent different fouling conditions encountered in the fields, a total of three fouling levels (i.e., VCI of 10%, 20%, 40%) were considered in this study. A precise amount of coal fouling was then introduced into the voids of ballast assembly.

A linear contact model was employed to simulate the interaction between ballast particles and coal fines. The micromechanical parameters of the contact model as listed in Table 1 were calibrated by DST on clean and coal-fouled ballast. Details of the parameter calibration can refer to a previous study [13] carried out by the authors.

The breakage of ballast was achieved by incorporating a clump-based degradation model developed by the authors [14, 15]. This degradation model can simulate the corner abrasion and surface attrition behavior of ballast particles.

Table 1. Micromechanical parameters of linear contact models.

Parameters	Values
Particle density	2750 (ballast)/ 1500 (coals) (kg/m^3)
Normal and shear contact stiffness for ballast, k_{nb}, k_{sb}	1.7×10^8 (N/m)
Normal and shear contact stiffness for coals, k_{nc}, k_{sc}	2.8×10^7 (N/m)
Normal and shear contact stiffness for walls, k_{nw}, k_{sw}	3.3×10^8 (N/m)
Friction coefficient for ballast, coals, and walls, μ_b, μ_c, μ_w	0.7 (ballast)/ 0.3 (coals)/ 0.1 (walls)

2.2 Test program

Prior to any loading, an initial load (q_{min}) of 45 kPa representing in-situ stress state was applied to the track assembly via sleeper wall. Three different cyclic loadings with the maximum stress (q_{max}) of 230 kPa, 370 kPa, and 420 kPa were then applied at a frequency of 15 Hz. These stress levels can be induced by trains with axle loads of 25 tonnes to 40 tonnes in the field. It should be noted that millions of cycles are required to for ballast to shakedown; however, the limited number of large asperities of clump particles and the overlooking of fatigue effect accelerated the DEM simulation to stabilize quickly compared to the laboratory experiments as well as to the field cases. Through a series of preliminary tests, it has been found that the accumulative settlement of ballast layer has become stable after 1000 cycles. Therefore, a total of 1000 cycles were applied for each specimen in this study.

2.3 Model validation

Fig. 2(a) shows the accumulative settlement of sleeper at the q_{max} of 420 kPa as loading progresses for clean and coal-fouled ballasted tracks. Here the accumulative settlement of sleeper (S) was normalized by the width of sleeper (B =300 mm). The loading cycle (N) was normalized by the total number of loading cycles (N_{max} =1000). It is seen that the settlement of sleeper accumulated faster within the initial 0.4 times N/N_{max}, after which it increased at an insignificant rate with number of loading cycles. This trend is consistent with that observed in the laboratory experiments by Indraratna et al. [16].

The ultimate settlements of sleeper (S_u) for ballasted tracks at varying VCI levels were shown in Fig. 2(b). The S_u measured in laboratory experiments by existing studies [16–19] have also been included in the figure for comparison. As expected, the S_u increased with the fouling level of the ballasted track bed increased. For the clean ballasted track, it attained a S_u of approximate 12 mm to 20 mm; however, the S_u increased to around 16 mm to 24 mm as the VCI of the track increased to 40%. The detrimental effect of fouling fines to the settlement of sleeper has also been observed by Indraratna et al. [16] in their laboratory experiments. In addition, the ultimate settlement of clean tracks measured by the current DEM model was in a closing range as that by previous studies [16–19], which also indicated the capability of the model in capturing the deformation response of ballasted tracks.

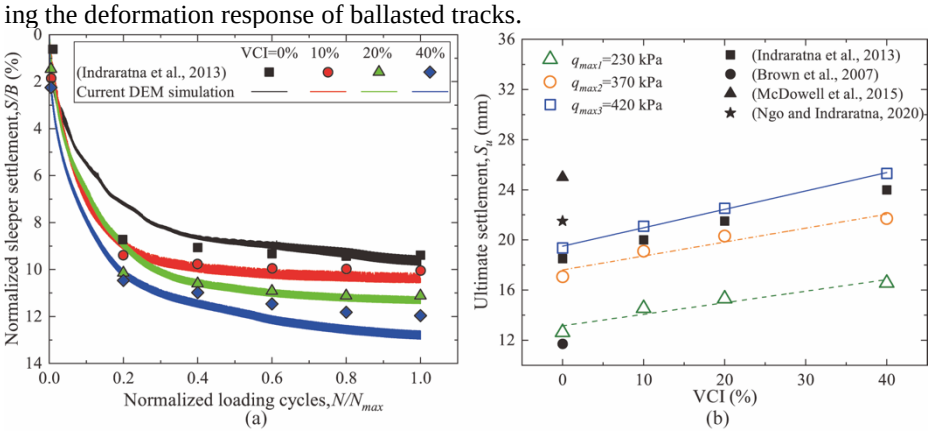

Fig. 2. (a) the accumulative settlement of sleeper in clean and fouled ballast tracks at the q_{max} of 420 kPa; (b) the ultimate sleeper settlement of ballasted tracks under various VCI levels

3 Results and Discussions

3.1 Ballast breakage

The breakage of ballast particles was simulated by the abrasion of sub-pebbles from their parent clumps, with the ballast debris being represented by newly-introduced fragment ball elements. The number of ballast fragments (B_f) with loading cycles (N) at the q_{max} of 420 kPa for ballasted tracks with varying VCI levels were shown in Fig. 3.

It is seen that most ballast breakage occurred within the initial 400 loading cycles, after which the assemblies experienced slight increases in B_f. Initially, ballast particles underwent rearrangement and compaction in response to cyclic loading, during which their likelihood of breakage was significantly elevated. This initial cyclic densification and breakage of ballast largely contribute to the settlement of the sleeper.

When it comes to the effect of fouling on the breakage of ballast, a reduced value of B_f was observed as the VCI of the ballasted track increased. The B_f of the clean ballasted tracks was around 200, while this value decreased by 50% when the VCI of the ballasted track increased to 40%. The mitigation of ballast breakage in fouled ballasted tracks was owing to the coating effect provided by the fouling fines. This finding was consistent with that observed in the laboratory study by Indraratna et al. [16].

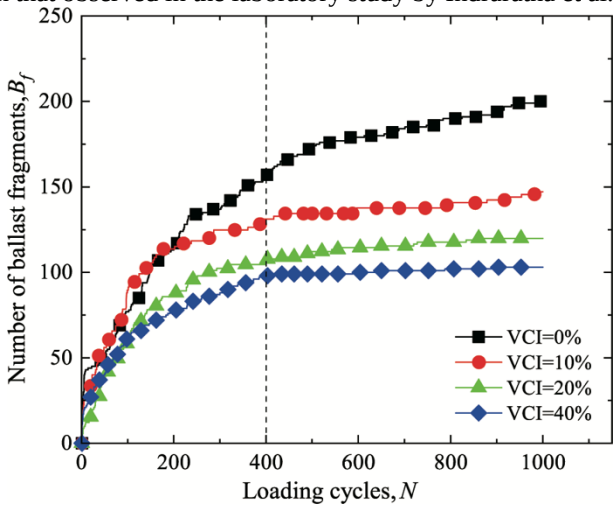

Fig. 3. The evolution of number of ballast fragments with loading cycles in clean and fouled ballasted tracks at the q_{max} of 420 kPa

Fig. 4 shows the distribution of ballast fragments along the longitude direction at the end of loading when subjected to a q_{max} of 420 kPa. It is seen that the ballast fragments were mainly distributed within a trapezoidal region underneath the sleeper, albeit a small amount was observed in the area of crib ballast. This is expected as the ballast underneath sleeper majorly develop higher contact force than crib ballast during cyclic loading. It is noteworthy that the delineated trapezoidal region aligned with the sleeper/ballast contact pressure zone identified in the ballast vibration modeling conducted by Ahlbeck [20]. A core degradation zone (CDZ), housing over 80% of the total broken fragments, was identified, as depicted in Fig. 4. As the VCI increased, the area of the CDZ within the ballasted tracks expanded, signifying a broader region influenced by fouling fines in relation to ballast breakage.

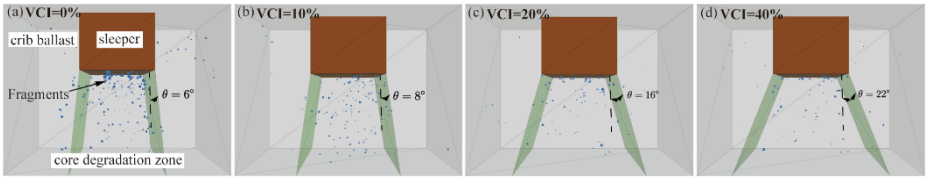

Fig. 4. The distribution of ballast fragments after loading in clean and fouled ballasted tracks at the q_{max} of 420 kPa

The fragmentation of ballast throughout the track depth was also investigated. Fig. 5 shows the number of ballast fragments (B_f) at various depths in both clean and fouled ballasted tracks at the end of loading under a q_{max} of 420 kPa. Notably, more than 80% of ballast fragments were concentrated within 0.6 times the z/h from the sleeper bottom, with a diminishing trend in B_f observed along the depth of the ballasted tracks. Here, h represented the thickness of the track bed, set at 300 mm in the current DEM analysis. Consequently, a critical degradation depth, estimated to be approximately 180 mm, emerged as a significant parameter for clean ballasted tracks. However, this critical degradation depth decreased to around 60 mm when the VCI of the track increased to 40%. The above findings suggest that different maintenance program be assigned to clean and fouled ballasted tracks.

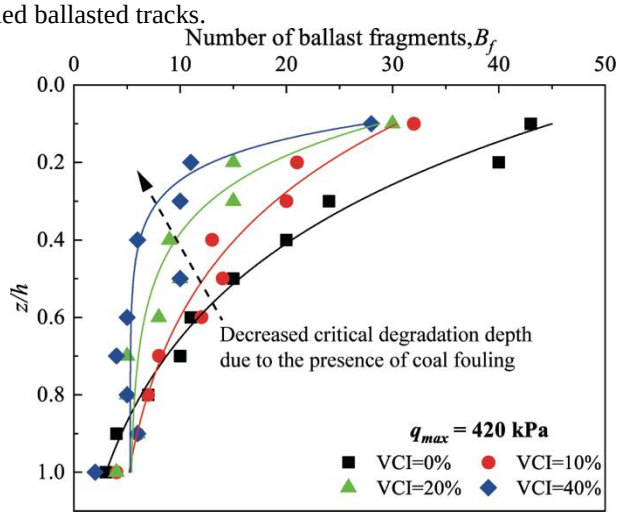

Fig. 5. The distribution of ballast fragments along track depth after loading in clean and fouled ballasted tracks at the q_{max} of 420 kPa

3.2 Resilient modulus of the track bed

The resilient modulus (M_R) is a critical parameter quantifying the deformation characteristics of track beds. It is defined as the ratio of the difference between q_{max} and q_{min} to the recoverable (resilient) strain ε_r. Here the strain was calculated by the settlement of sleeper (S) to the thickness of the track bed (h). Fig. 6 shows the M_R of clean and fouled ballasted tracks when under various q_{max} values. As expected, a slight increase

was observed in the M_R with the increase in q_{max} for both fresh and fouled ballasted tracks. A significant drop in M_R was observed when the track bed was at higher fouling levels. For clean ballasted tracks (VCI= 0%), the M_R was around 138 MPa and 150 MPa under the q_{max} of 230 kPa and 420 kPa, respectively; however, this value decreased to around 75 MPa and 90 MPa, respectively, for the fouled ballasted tracks with a VCI of 40%. This observation implied the profound influence of the clogged fouling fines on the ability of deformation recovery of ballasted tracks.

Based on the simulation results, a formula relating M_R with VCI and q_{max} was established, as given by Eq. (2),

$$M_R = a_1 \times a_2^{\mathrm{VCI}} + b \times q_{max} + c \tag{2}$$

where $a_1 = 72.97$, $a_2 = 0.95$, $b = 0.07$, $c = 47.36$.

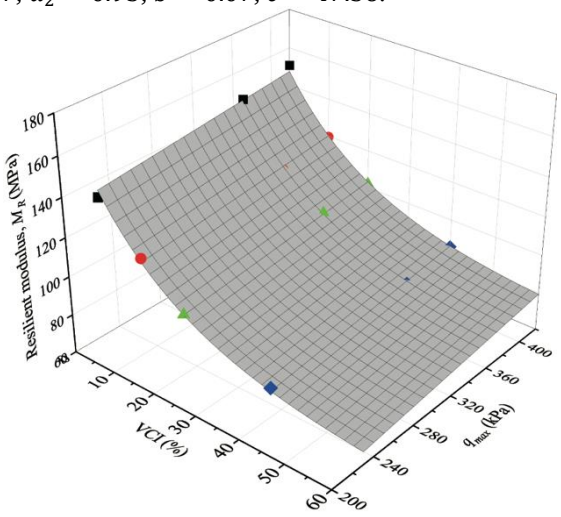

Fig. 6. The relationship between resilient modulus of ballasted tracks with fouling level VCI and the maximum deviatoric stress q_{max}

3.3 Micromechanical response of the track bed

Leveraging the DEM modeling, the micromechanical responses in terms of the intensity and anisotropy of inter-particle contacts were also explored.

Fig. 7 shows the evolution of coordination number (Z) with loading cycles (N) in ballast aggregates under a q_{max} of 420 kPa for ballasted tracks having different fouling levels. It is seen that the values of Z increased rapidly within the initial 400 loading cycles for both clean and fouled ballasted tracks, which was because ballast aggregates became densified through cyclic loading. Beyond this, the Z was maintained at a constant level, albeit some fluctuations. The ultimate value of Z for clean ballasted tracks was around 5.75, while it decreased to around 4.9 when the VCI of the track increased to 40%. This phenomenon is known as the 'coating effect' of fouling fines, which coated the surface of ballast particles, and hence imparted their inter-particle interactions.

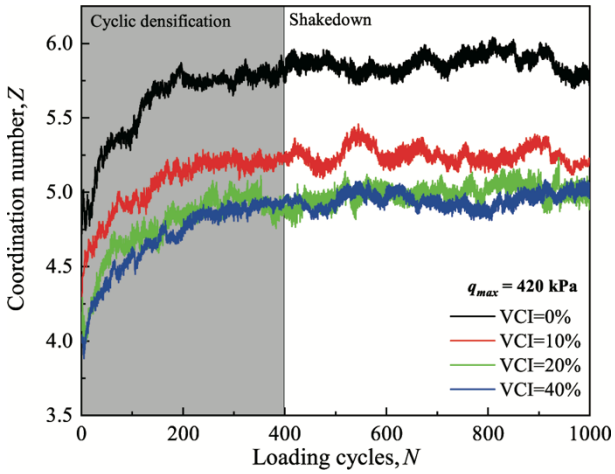

Fig. 7. Evolution of coordination number in clean and fouled ballast at the q_{max} of 420 kPa

Fig. 8 shows the averaged interparticle contact force (f_{ave}) measured at different depths of ballasted tracks at the end of loading when under a q_{max} of 420 kPa. With the increase of z/h, the f_{ave} became attenuated. Consequently, the possibility of ballast breakage was reduced. It is also found that the f_{ave} of the clean ballasted tracks was greater than that of the fouled ones at all depths. The decrease in contact intensity observed in fouled ballasted tracks, represented by a reduced value of coordination number Z and averaged interparticle contact forces f_{ave}, explained their mitigation of ballast breakage in comparison to clean ones.

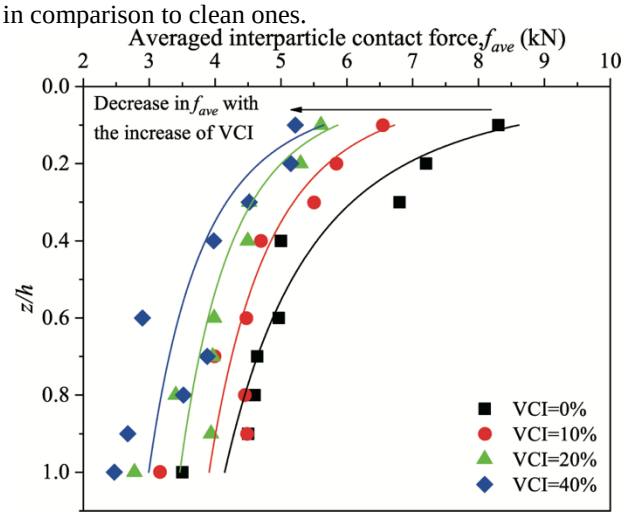

Fig. 8. The averaged interparticle contact forces at varying track depths after loading at the q_{max} of 420 kPa

Fig. 9 shows the distribution of interparticle contacts for clean and fouled ballasted tracks at the end of loading when under a q_{max} of 420 kPa. The contact forces were

represented by lines connecting the centroids of ballast particles with the line thickness being scaled by its magnitude. It is seen that the traffic load was mainly supported by bottom ballast, as the interparticle contact forces in this area exhibited relatively larger values compared to those in the cribs. The interparticle contact forces were transmitted within a trapezoidal region underneath sleeper. It is also noteworthy that the trapezoidal distributions of interparticle contact force nearly coincided with the distributions of ballast fragments as shown in Fig. 4., which explained the emergence of core degradation zone underneath sleeper.

The anisotropy of interparticle contact forces was quantified by using a fabric tensor based on contact forces [21], as given by Eq. (3),

$$F_{ij} = \frac{1}{N_c}\sum_{c=1}^{N_c} f_i^k f_j^k \tag{3}$$

where f^k is unit contact forces, N_c is the number of interparticle contacts. The anisotropy a_f can be calculated by considering the largest and smallest eigenvalues of **F** ($F_1 > F_3$), as given by Eq. (4).

$$a_f = \ln F_1 - \ln F_3 \tag{3}$$

The a_f for clean and fouled ballasted tracks were provided in Fig. 9. A diminished a_f was observed with the increase of VCI, signifying a more isotropic distribution of interparticle contact forces between bottom ballast. These less intensified interparticle contact forces also contribute to the mitigation of ballast breakage occurred in fouled ballasted tracks.

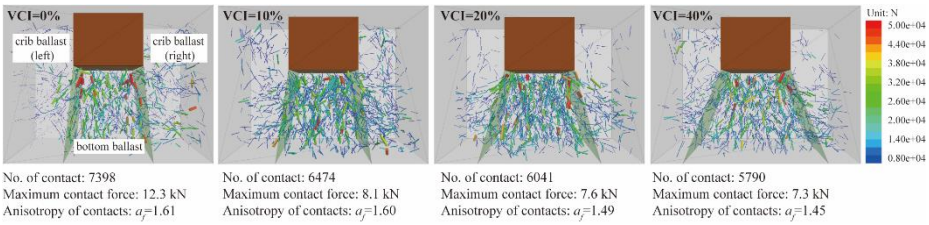

Fig. 9. The distribution of interparticle contacts for clean and fouled ballasted tracks after loading at the q_{max} of 420 kPa

4 Conclusions

The impact of coal fouling on the deformation and degradation behavior of ballast aggregates in ballasted tracks has been investigated using DEM modeling. Simulations were conducted on representative sections of ballasted tracks, each containing one sleeper and real-shaped ballast aggregates contaminated with varying amounts of coal fines. Different cyclic loading scenarios representing various axle wheel loads were applied to these ballast assemblies. The study explored parameters such as sleeper settlement, track bed resilient modulus, and ballast particle breakage for ballasted tracks with different levels of fouling. Additionally, the micromechanical response, including coordination number and interparticle contact network, was analyzed to gain insights into the fundamental mechanisms of fouling effects on ballasted tracks. The main conclusions are summarized as follows:

(1) Upon cyclic loading, ballast aggregates were compacted and rearranged, during which significant particle breakage occurred. The cyclic densification of the aggregates and the breakage of ballast particles contributed to the rapid increase of sleeper settlement.
(2) Coal fouling detrimentally increased the sleeper settlement and reduced the resilient modulus of track beds. The resilient modulus of clean ballasted tracks under the q_{max} of 230 kPa and 420 kPa was around 138 MPa and 150 MPa, respectively; however, the resilient modulus decreased to around 75 MPa and 90 MPa, respectively, for the fouled ballasted tracks with a VCI of 40%.
(3) With the increase of fouling level, the breakage of ballast particles became mitigated owing to the 'coating effect' provided by coal fouling, which reduced the amount of interparticle contacts and the contact forces between ballast particles.
(4) The breakage of ballast particles reduced along track depths. Beyond a depth of 180 mm, the damage to fresh ballast was insignificant, and this critical depth decreases to around 90 mm for ballast at VCI of 40%.

References

1. Tennakoon N, Indraratna B, Rujikiatkamjorn C, et al (2012) The Role of Ballast-Fouling Characteristics on the Drainage Capacity of Rail Substructure. Geotech Test J 35:629–640

2. Tennakoon NC, Indraratna B (2014) Behaviour of clay-fouled ballast under cyclic loading. Géotechnique 64:502–506. https://doi.org/10.1680/geot.13.T.033

3. Huang H, Tutumluer E, Dombrow W (2009) Laboratory Characterization of Fouled Railroad Ballast Behavior. In: Transportation Research Record. Salt Lake City, UT, pp 93–101

4. Tutumluer E, Kent PF, Dombrow W, Huang H (2008) Laboratory characterization of coal dust fouled ballast behavior. Salt Lake City, UT

5. Danesh A, Palassi M, Mirghasemi AA (2018) Effect of sand and clay fouling on the shear strength of railway ballast for different ballast gradations. Granul Matter 20:51. https://doi.org/10.1007/s10035-018-0824-z

6. Cundall PA, Strack ODL (1979) Discrete numerical model for granular assemblies. International Journal of Rock Mechanics and Mining Sciences & Geomechanics Abstracts 29:47–65. https://doi.org/10.1016/0148-9062(79)91211-7

7. Huang H, Tutumluer E (2011) Discrete Element Modeling for fouled railroad ballast. Constr Build Mater 25:3306–3312. https://doi.org/10.1016/j.conbuildmat.2011.03.019

8. Indraratna B, Ngo NT, Rujikiatkamjorn C, Vinod JS (2014) Behavior of Fresh and Fouled Railway Ballast Subjected to Direct Shear Testing: Discrete Element Simulation. International Journal of Geomechanics 14:34–44. https://doi.org/10.1061/(ASCE)GM.1943-5622.0000264

9. Ngo NT, Indraratna B, Rujikiatkamjorn C (2014) DEM simulation of the behaviour of geogrid stabilised ballast fouled with coal. Comput Geotech 55:224–231. https://doi.org/10.1016/j.compgeo.2013.09.008

10. Chen J, Indraratna B, Vinod JS, et al (2021) Stress-dilatancy behaviour of fouled ballast: experiments and DEM modelling. Granular Matter 23:90. https://doi.org/10.1007/s10035-021-01150-1

11. Xu Y, Gao L, Zhang Y, et al (2016) Discrete element method analysis of lateral resistance of fouled ballast bed. J Cent South Univ 23:2373–2381. https://doi.org/10.1007/s11771-016-3296-5

12. Indraratna B, Salim W, Rujikiatkamjorn C (2011) Advanced Rail Geotechnology - Ballasted Track. CRC Press, Taylor & Francis Group, London, UK

13. Chen J, Gao R, Liu Y, et al (2021) Numerical exploration of the behavior of coal-fouled ballast subjected to direct shear test. Construction and Building Materials 273:121927. https://doi.org/10.1016/j.conbuildmat.2020.121927

14. Liu Y, Gao R, Chen J (2021) A new DEM model to simulate the abrasion behavior of irregularly-shaped coarse granular aggregates. Granular Matter 23:61. https://doi.org/10.1007/s10035-021-01130-5

15. Chen J, Vinod JS, Indraratna B, et al (2022) A discrete element study on the deformation and degradation of coal-fouled ballast. Acta Geotech 17:3977–3993. https://doi.org/10.1007/s11440-022-01453-4

16. Indraratna B, Ngo NT, Rujikiatkamjorn C (2013) Deformation of Coal Fouled Ballast Stabilized with Geogrid under Cyclic Load. J Geotech Geoenviron Eng 139:1275–1289. https://doi.org/10.1061/(ASCE)GT.1943-5606.0000864

17. Brown SF, Kwan J, Thoma NH (2007) Identifying the key parameters that influence geogrid reinforcement of railway ballast. Geotext Geomembr 25:326–335. https://doi.org/10.1016/j.geotexmem.2007.06.003

18. Ngo T, Indraratna B (2020) Mitigating ballast degradation with under-sleeper rubber pads: Experimental and numerical perspectives. Computers and Geotechnics 122:103540. https://doi.org/10.1016/j.compgeo.2020.103540

19. McDowell GR, Lim WL, Collop AC, et al (2005) Laboratory simulation of train loading and tamping on ballast. Proceedings of the Institution of Civil Engineers 158:89–95

20. Ahlbeck DR, Meacham HC, Prause RH (1978) THE DEVELOPMENT OF ANALYTICAL MODELS FOR RAILROAD TRACK DYNAMICS. In: Railroad Track Mechanics and Technology. Elsevier, pp 239–263

21. Ouadfel H, Rothenburg L (2001) `Stress–force–fabric' relationship for assemblies of ellipsoids. Mechanics of Materials 33:201–221. https://doi.org/10.1016/S0167-6636(00)00057-0